ORGANOMETALLICS

Article

pubs.acs.org/Organometallics

# Computational Study on the C−Heteroatom Bond Formation via Stille Cross-Coupling Reaction: Differences between Organoheterostannanes $Me_3SnAsPh_2$ vs $Me_3SnPPh_2$

E. Daiann Sosa Carrizo,[†] Israel Fernández,*[,‡] and Sandra E. Martín*[,†]

[†]Departamento de Química Orgánica, Facultad de Ciencias Químicas, INFIQC (CONICET−Universidad Nacional de Córdoba), Medina Allende y Haya de la Torre, X5000HUA, Córdoba, Argentina

[‡]Departamento Química Orgánica I, Facultad de Ciencias Químicas, Universidad Complutense Madrid, 28040, Madrid, Spain

Supporting Information

**ABSTRACT:** The formation of C−heteroatom bonds through the Stille cross-coupling reaction has been explored computationally within the density functional theory framework. To this end, the reaction profiles of the processes involving different aryl halides (PhCl, PhI) and heterostannanes ($Me_3SnZR_2$, Z = As, P; R = Ph, Me) in the presence of palladium catalyst have been investigated and compared to gain more insight into the differential reactivity observed experimentally. In addition, the main features of the reaction steps where the heterostannanes are involved, namely, the transmetalation and reductive elimination reactions, have been analyzed in detail. It was found that the overall relative reaction profile for the transmetalation step involving heterostannanes with Z = P is energetically favored over that involving species having Z = As, which agrees with the experimental observations. This can be mainly ascribed to the relative strength of the Sn−Z bond, which is broken during the transmetalation step (Sn−P < Sn−As).

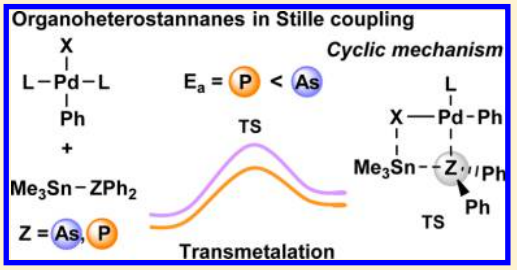


## INTRODUCTION

Nowadays, palladium-catalyzed cross-coupling reactions are well-established methods for the formation of C−C bonds, having found widespread applications in the preparation of a wide range of compounds and materials.[1] The Stille reaction,[2] i.e., the transition-metal-catalyzed cross-coupling of organostannanes with organic electrophiles, is one of these versatile methods that have achieved wide recognition as an exceptionally mild and efficient reaction. For that reason, the Stille coupling has become a popular tool in practical organic synthesis, with applications in drug discovery,[3] natural products synthesis,[4] materials chemistry, and other fields.[5]

Interestingly, the scope of the Stille reaction is not exclusively limited to the formation of new C−C bonds. Indeed, heteroatom-containing stannanes have been employed as nucleophiles in cross-coupling reactions for the formation of C−N, C−P, C−Se, C−S, and C−Sn bonds.[6] Accordingly, we have developed a versatile methodology that leads to C−heteroatom bond formation through a Stille Pd-catalyzed cross-coupling reaction of different electrophiles with organoheterostannanes of the type $R_3SnZPh_n$ (Z = P, Se) in a one-pot, two-step reaction (Scheme 1).[7] Following this methodology, we have described for the first time the C−As bond formation by the Pd-catalyzed reaction of different electrophiles with arsine stannane *n*-$Bu_3SnAsPh_2$ (**A**) (Scheme 1).[7c,8] In addition, this procedure has been helpful toward the synthesis of functionalized triarylarsines and arsine ligands.[8b,9] Both the Pd-catalyzed arsination and phosphination reactions could be carried out using a wide variety of aryl iodides, including those sterically hindered, in the presence of different functional groups and achieving high yields of the corresponding coupling product.[7a,c,d,8] However, it was not possible to successfully accomplish similar transformations involving aryl bromides and chlorides under many tested reaction conditions, including those in which these halides have proven to produce new C−C bonds. It becomes therefore clear that a comprehensive understanding on how organoheterostannanes can affect the catalytic cycle of the Stille reaction is crucial to continue improving the applicability of these reactions.

The mechanism of the Stille reaction has been continuously investigated since its discovery and after the simplified mechanism originally proposed by Stille.[10] Although the classical widely accepted mechanisms proceed via three fundamental steps prevalent in transition-metal-catalyzed C−

**Scheme 1. Experimentally Studied Stille Reactions Involving Heterostannanes**[a]

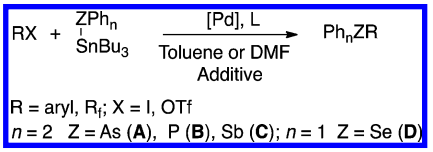


[a]See refs 7−9.

**Received:** October 8, 2014

  

DOI: 10.1021/om501027s
*Organometallics* XXXX, XXX, XXX−XXX

C bond-forming reactions, namely, oxidative addition, transmetalation, and reductive elimination (Figure 1), the process

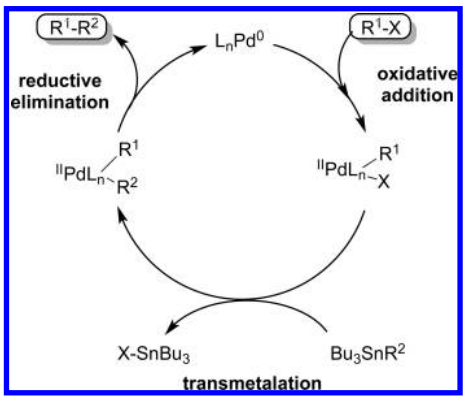


**Figure 1.** Widely accepted reaction mechanism for the Stille reaction.

itself is known to be far more complex. Variation in reaction conditions (i.e., electrophile, ligands, solvents, Pd source, additives, etc.) has played a key role in the outcome of the Stille reaction, and for that reason alternative mechanistic pathways have been suggested.[2a] Extensive experimental[11] and computational studies[12] have corroborated or modified the different mechanistic proposals, thus enhancing our current understanding of this fascinating and synthetically useful transformation.

Despite the broad amount of mechanistic studies focused on the Stille C−C bond-forming reaction, to the best of our knowledge, the effect of organoheterostannanes on the catalytic cycle has not been considered so far. Such a study is needed to understand the role of these particular stannanes in the transformation and in order to design new, more efficient processes. Taking into account our previous experimental results,[7−9] herein a computational study on the complete catalytic cycle for the Stille reaction involving organoheterostannanes derived from As and P (**A**, **B**; see Scheme 1) and aryl halides is reported. The transmetalation and the reductive elimination reactions, where the influence of the stannane-transferring group $-AsPh_2$ and $-PPh_2$ should be greater, will be analyzed in detail.

## RESULTS AND DISCUSSION

**Overall Reaction Profile.** Before going into detail, the following experimental finding should be highlighted first. It was found that, under the same reaction conditions, the phosphorus heterostannane *n*-$Bu_3SnPPh_2$ (**B**) leads to higher conversions and isolated reaction yields than the As counterpart *n*-$Bu_3SnAsPh_2$ (**A**) in the cross-coupling reaction with aryl iodides catalyzed by $(Ph_3P)_2PdCl_2$.[7a,8] As shown in Scheme 2, higher reaction yields were systematically achieved when using phosphorus stannane **B** compared to stannane **A** in the processes involving 1-chloro-4-iodobenzene and 1-iodonaphthalene in toluene at the same temperature and reaction times.

Density functional theory (DFT) calculations have been carried out at the PCM(toluene)-B3LYP-D3/6-311+G(d)&SDD//B3LYP/6-31+G(d)&SDD level (see Computational Details) to gain more insight into the observed different reactivity of organoheterostannanes **A** and **B**. The corresponding computed reaction profiles of the cross-coupling reaction of phenyl iodide (**1a**) and the model heterostannanes $Me_3SnAsPh_2$ (**A′**) and $Me_3SnPPh_2$ (**B′**), where the *n*-butyl

**Scheme 2. Stille Reactions of 1-Chloro-4-iodobenzene and 1-Iodonaphthalene with Heterostannanes**

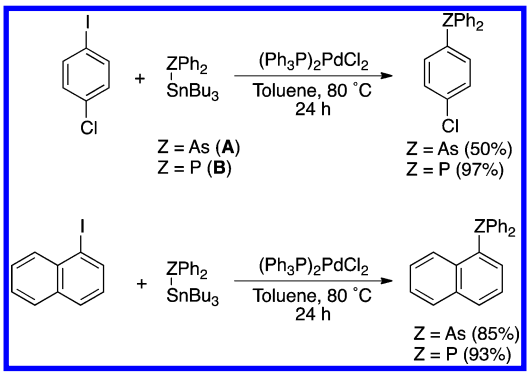


groups in **A** and **B** were replaced by methyl groups, in the presence of the model active catalyst $Pd(PMe_3)_2$ are depicted in Figure 2, which gathers the computed relative free energies ($\Delta G_{298}$, at 298.15 K) using toluene as the solvent.

The process begins with the oxidative addition of PhI (**1a**) to $Pd(PMe_3)_2$. As previously reported,[12b,13,14] the transformation starts from the initial Pd(0)-$\pi$-complex **2a**, which is then transformed into the Pd(II) complex ***cis*-3a** in a highly exergonic transformation ($\Delta G_{R,298}$ = −24.1 kcal/mol).[15] This step occurs concertedly through the typical three-membered transition state **TS2a**,[16] which is associated with the simultaneous formation of the Pd−C and Pd−X bonds. Similar to related oxidative addition processes,[15] intermediates ***cis*-3a** readily isomerizes to the most stable ***trans*-4a**, which lies 10.4 kcal/mol below ***cis*-3a** (Figure 2).

From intermediate ***trans*-4a**, the subsequent transmetalation reaction occurs. Two main alternative pathways have been suggested for this reaction step to account for the reported experimental evidence:[2a] (i) the open mechanism, where the transmetalation process occurs via the replacement of the leaving group X (in this case, X = I) by a neutral ligand followed by an $S_N2$ substitution reaction of a ligand by the stannane group with the previously dissociated $X^-$ as the incoming group, and (ii) the cyclic mechanism, which involves a four-membered transition state resulting in the replacement of a ligand by the stannane-transferring substituent. It is generally accepted that the open mechanism will prevail whenever two ancillary ligands, usually phosphines or arsines, remain attached to palladium in the key transition state, while the cyclic mechanism will dominate when one ligand is released during the process.[12b,17] Moreover, the cyclic pathway is favored for the coupling of X-bridging electrophiles such as halides in nonpolar solvents. Indeed, our calculations indicate that the first step of the possible open mechanism, which involves the replacement of the iodide ligand by a phosphine (in our case, $PMe_3$) to form the cationic $PhPd(PMe_3)_3^+$ complex,[17b] is highly endergonic ($\Delta G_{R,298}$ = +31.3 kcal/mol). This suggests that the open mechanism is not competitive in these particular reaction conditions (phenyl iodide and toluene as the solvent).

Therefore, we then focused on the transmetalation reaction via the so-called cyclic reaction mechanism. The process starts with the $PMe_3$ by $Me_3SnZPh_2$ substitution, which transforms ***trans*-4a** into intermediates **5a**. This process very likely takes place through an associative mechanism similar to that reported for related transmetalations.[17b] Not surprisingly, the $Me_3P$/$Me_3SnAsPh_2$ ligand interchange is endergonic, whereas the


DOI: 10.1021/om501027s
Organometallics XXXX, XXX, XXX−XXX

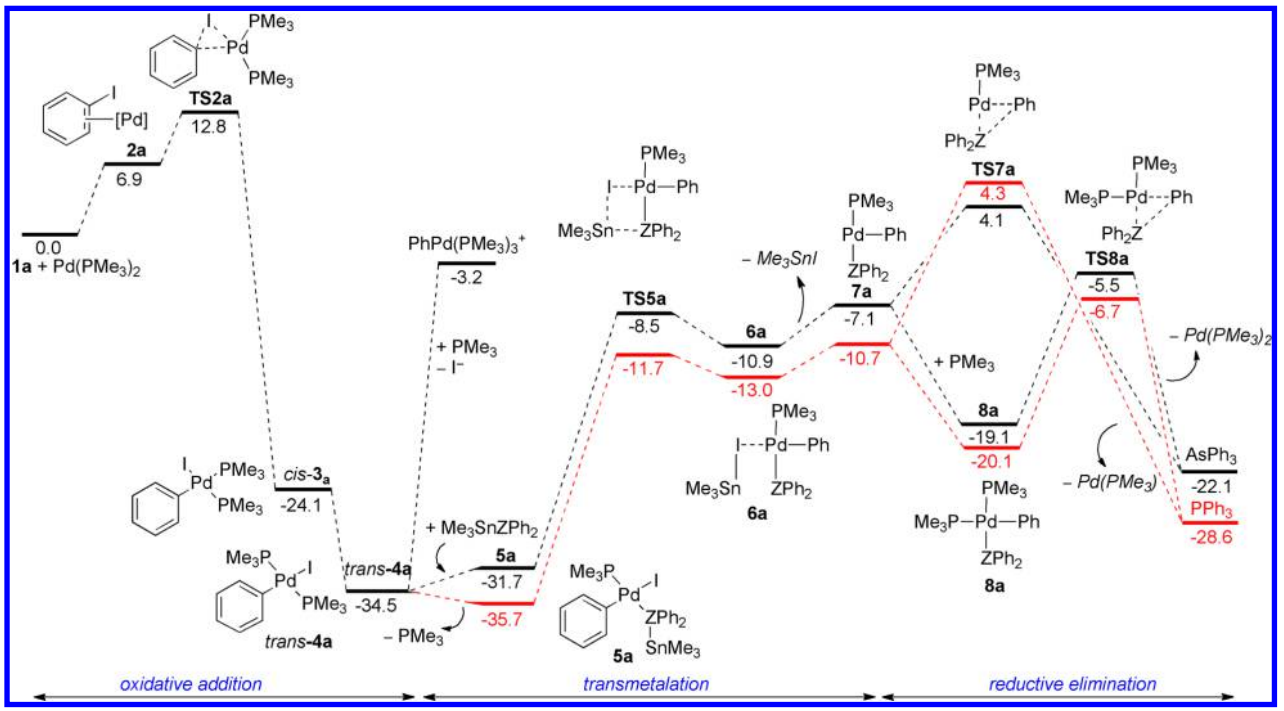


**Figure 2.** Computed reaction profile for the whole catalytic cycle of the Stille cross-coupling reaction of PhI (**1a**) and $Me_3SnAsPh_2$ (**A′**, black line) and $Me_3SnPPh_2$ (**B′**, red line) catalyzed by $Pd(PMe_3)_2$. Relative free energies ($\Delta G_{298}$, at 298.15 K) are given in kcal/mol. All data have been computed at the PCM(toluene)-B3LYP-D3/6-311+G(d)&SDD//B3LYP/6-31+G(d)&SDD level.

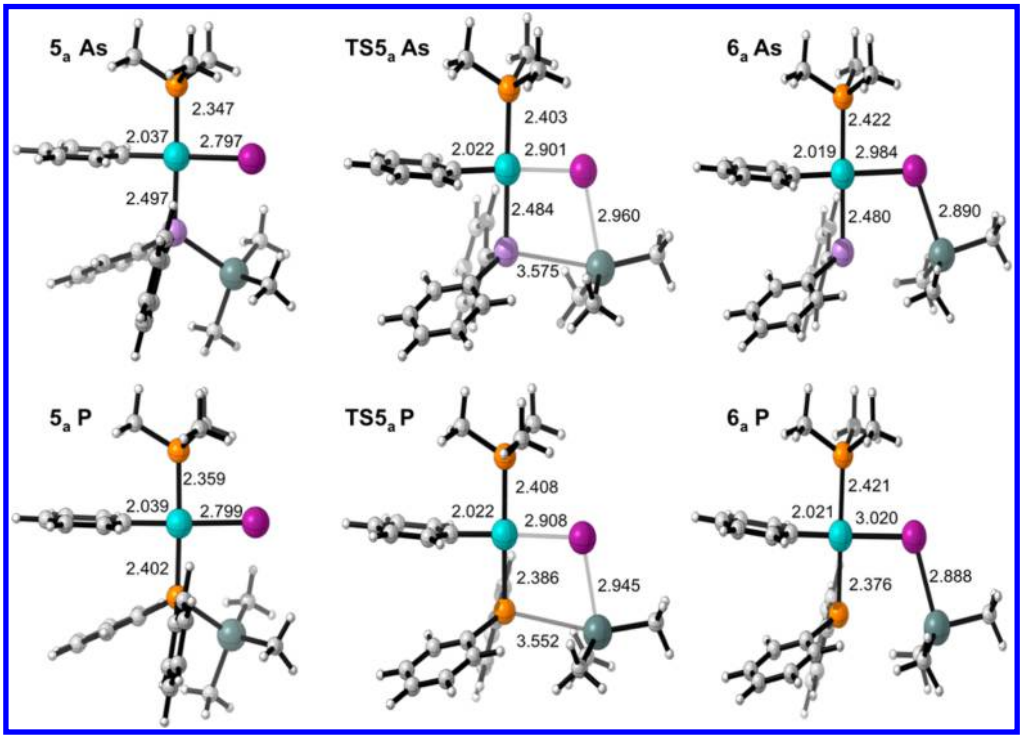


**Figure 3.** Ball-and-stick representations of the species involved in the transmetalation reaction of **5a** into **6a**. All structures correspond to fully optimized B3LYP/6-31+G(d)&SDD geometries. Bond distances are given in angstroms.

$Me_3P/Me_3SnPPh_2$ interchange is slightly exergonic as a result of the relative $\sigma$-donor ability of the ligands ($Me_3SnPPh_2$ > $Me_3SnAsPh_2$). Indeed, our calculations indicate that the corresponding Z lone-pair, which corresponds to the HOMO of $Me_3SnZPh_2$, is more stabilized for Z = As (−5.72 eV) than for Z = P (−5.62 eV). This is translated into a more favorable HOMO−LUMO interaction between $Me_3SnZPh_2$ and the Pd(II) complex for Z = P, which is reflected in the exergonicity computed for the process involving $Me_3SnPPh_2$ (see Figure 2).

From **5a**, the second step of the transmetalation reaction takes place. This process involves the four-membered cyclic transition state **TS5a**, which is associated with the simultaneous Sn−I bond formation and Sn−Z and Pd−I bond breaking (see Figure 3). Interestingly, the computed relative activation



DOI: 10.1021/om501027s
*Organometallics* XXXX, XXX, XXX−XXX

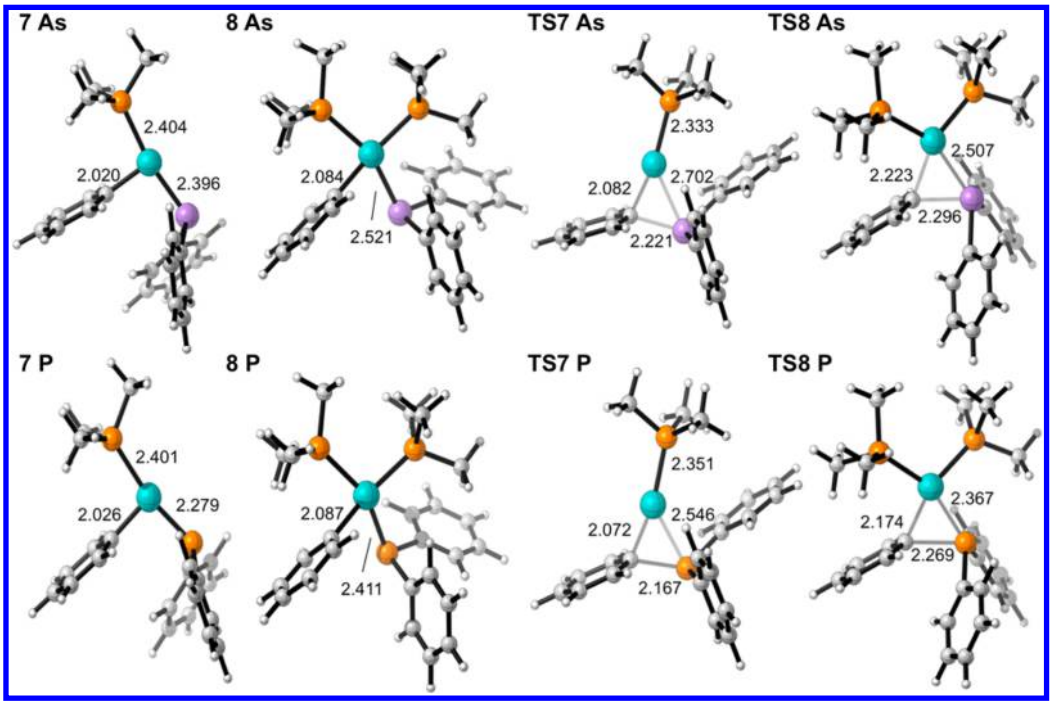


**Figure 4.** Ball-and-stick representations of the species involved in the reductive elimination reaction of **7a**. All structures correspond to fully optimized B3LYP/6-31+G(d)&SDD geometries. Bond distances are given in angstroms.

barriers are quite similar for Z = As, P ($\Delta G^{\ddagger}_{298}$ = 23.2 kcal/mol for Z = As, and $\Delta G^{\ddagger}_{298}$ = 24.0 kcal/mol for Z = P). Despite that, the overall relative reaction profile for the transmetalation involving $Me_3SnPPh_2$ is always energetically favored, which nicely agrees with the experimental observations.[7,8] This finding is directly related to the relative strength of the Sn−Z bond, which is broken during the **5a** → **TS5a** → **7a** transformation. Indeed, our calculations confirm that the Sn−P bond is more labile than the Sn−As bond in intermediates **5a** (corresponding Sn−Z Wiberg bond indices, WBI, of 0.65 and 0.69 for Z = P and Z = As, respectively). In addition, closer inspection of the transition states **TS5a** (Figure 3) suggests that the Sn···I bond is more developed in the process involving Z = P (Sn···I bond lengths of 2.945 and 2.960 Å, for **TS5a-P** and **TS5a-As**, respectively), thus indicating a stronger, i.e., more stabilizing, Sn···I interaction in **TS5a-P**. Both factors, namely, the Sn−Z bond strength and the Sn−I interaction in the cyclic transition state, contribute to the observed higher reactivity of the phosphorus-derived heterostannane. Finally, the high activation barrier and the high endergonicity computed for this two-step transmetalation reaction are also in agreement with the high temperatures (80 °C) required experimentally.

The process ends up with the irreversible reductive elimination step from the T-shaped tricoordinated intermediate **7a**, which leads to final reaction products ($PPh_3$ or $AsPh_3$; see Figure 2) via transition state **TS7a**. This saddle point is associated with the simultaneous formation of the new Z−$C_{aryl}$ bond and Pd−Z and Pd−$C_{aryl}$ bond ruptures (Figure 4). In this event, the computed activation barrier for the process involving Z = P ($\Delta G^{\ddagger}_{298}$ = 15.0 kcal/mol) is higher than that for the analogous reaction involving Z = As ($\Delta G^{\ddagger}_{298}$ = 11.2 kcal/mol). Again, this may be ascribed to the relative Pd−Z bond strengths in intermediate **7a** (the corresponding Pd−C bonds are quite similar; see Figure 4). This hypothesis is confirmed by the computed WBIs, which indicate that the Pd−P bond in **7a-P** is stronger than the Pd−As in **7a-As** (WBI = 0.83 and 0.79, respectively). Despite that, the process involving **7a-P** is clearly thermodynamically favored in view of the computed higher (i.e., more negative) reaction energies as compared to the analogous process involving **7a-As** ($\Delta\Delta G_{R,298}$ = 2.9 kcal/mol). Although the reductive elimination step with organoheterostannanes is less exergonic than the respective process leading to C−C bond formation,[17,18] it compensates the previous endergonic transmetalation step and drives the complete catalytic cycle forward.

Alternatively, it can be suggested that coordinatively unsaturated complexes **7a** can coordinate a new phosphine ligand (which was released in the transmetalation step) to produce the tetracoordinated complexes **8a** prior to the reductive elimination.[19] As the initial coordination of the new $PMe_3$ ligand is highly exergonic ($\Delta G_{R,298}$ = −12.0 and −9.4 kcal/mol for Z = As and Z = P, respectively) and the associated barriers involving **TS8a** ($\Delta G^{\ddagger}_{298}$ = 13.6 kcal/mol for Z = As, and $\Delta G^{\ddagger}_{298}$ = 13.4 kcal/mol for Z = P) are comparable to those involving **TS7a** (see above), it can be concluded that this alternative reaction pathway is competitive toward the formation of the final products.

**Effect of the Halide.** Once the reaction profile for the Stille coupling involving heterostannanes has been established, we next turned our attention to the effect of the halide in the process to gain more insight into the experimentally observed lack of reactivity of aryl chlorides.[7,8] Figure 5 shows the corresponding computed reaction profile for the Pd-catalyzed cross-coupling reaction of phenyl chloride (**1b**) with $Me_3SnZPh_2$ (Z = As, P). Similarly, the transmetalation step, which again occurs via the cyclic mechanism in view of the high endergonicity ($\Delta G_{R,298}$ = +35.7 kcal/mol) associated with the $Cl^-/PMe_3$ ligand interchange, is clearly more favored for Z = P along the entire reaction coordinate, thus indicating that the main factor controlling this process is the relative Sn−Z bond strength (the Sn···Cl interaction in the corresponding transition states seems to be not that relevant; see Figure 6). Interestingly,


DOI: 10.1021/om501027s
Organometallics XXXX, XXX, XXX−XXX

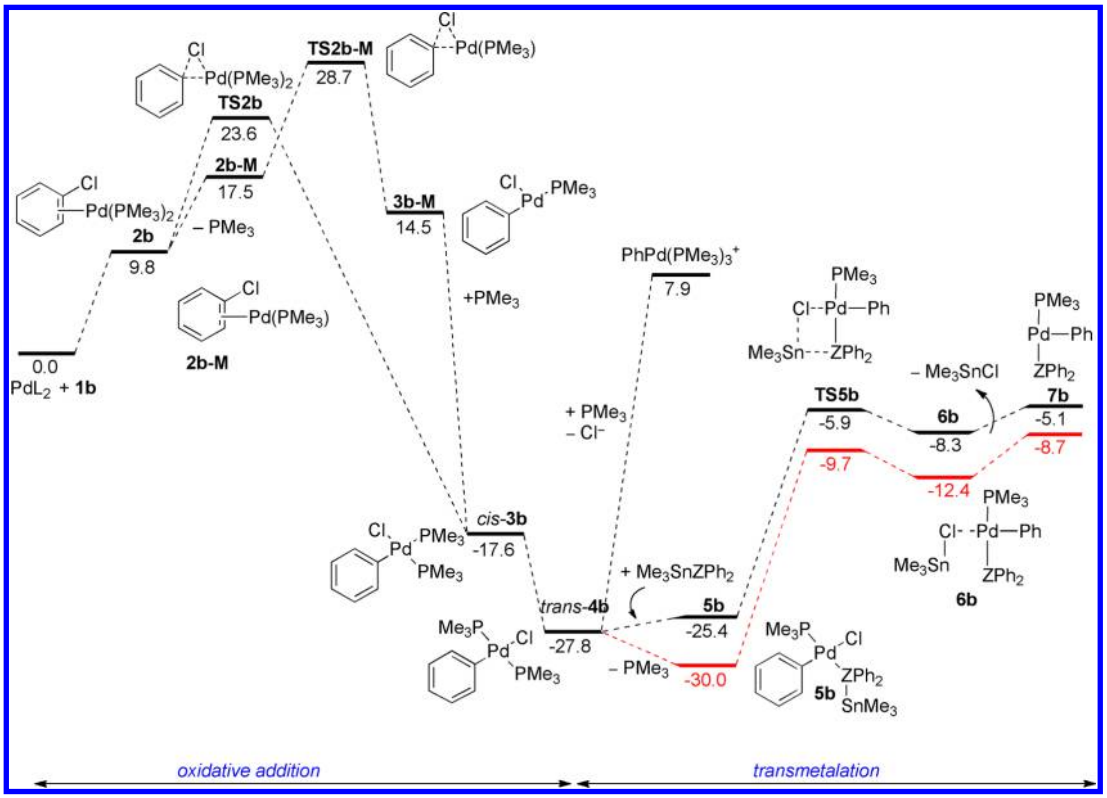


**Figure 5.** Computed reaction profile for the whole catalytic cycle of the Stille cross-coupling reaction of PhCl (**1b**) and $Me_3SnAsPh_2$ (**A′**, black line) and $Me_3SnPPh_2$ (**B′**, red line) catalyzed by $Pd(PMe_3)_2$. Relative free energies ($\Delta G_{298}$, at 298.15 K) are given in kcal/mol. All data have been computed at the PCM(toluene)-B3LYP-D3/6-311+G(d)&SDD//B3LYP/6-31+G(d)&SDD level.

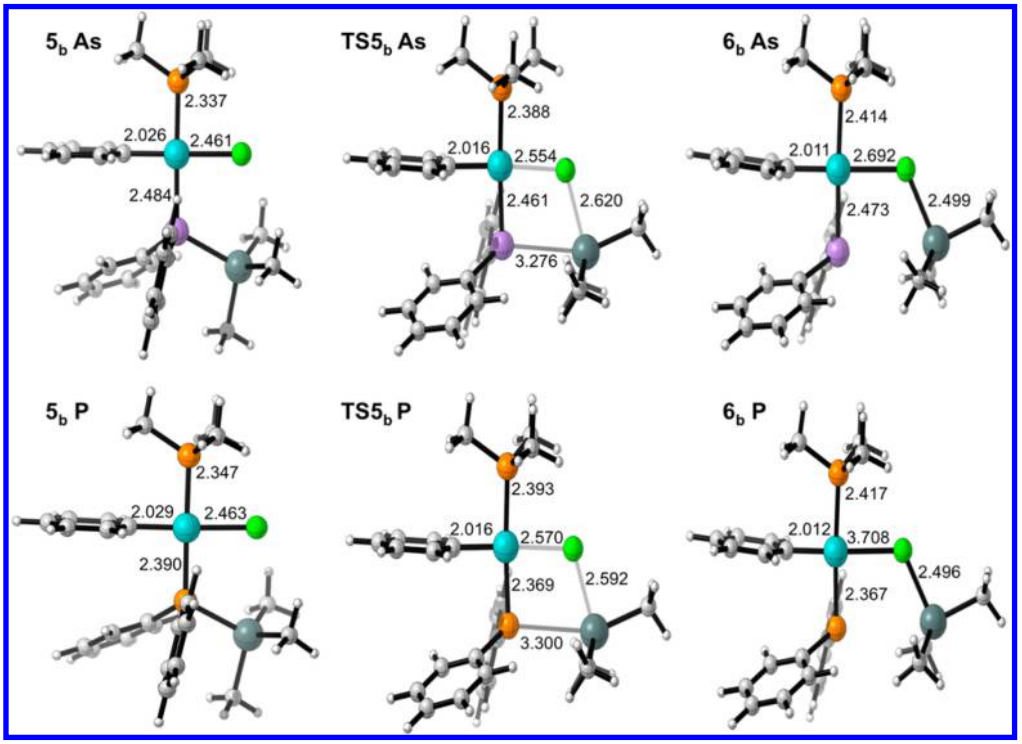


**Figure 6.** Ball-and-stick representations of the species involved in the transmetalation reaction of **5b** into **6b**. All structures correspond to fully optimized B3LYP/6-31+G(d)&SDD geometries. Bond distances are given in angstroms.

the computed activation barriers for the **5b** → **TS5b** → **7b** transformation ($\Delta G^{\ddagger}_{298}$ = 19.5 kcal/mol for Z = P, and $\Delta G^{\ddagger}_{298}$ = 20.3 kcal/mol for Z = As) are comparatively lower than those involving **TS5a** (see above, Figure 2). This result agrees with a previous DFT study on the effect of the leaving group X on the transmetalation of vinylstannanes, which found that the overall



DOI: 10.1021/om501027s
Organometallics XXXX, XXX, XXX–XXX

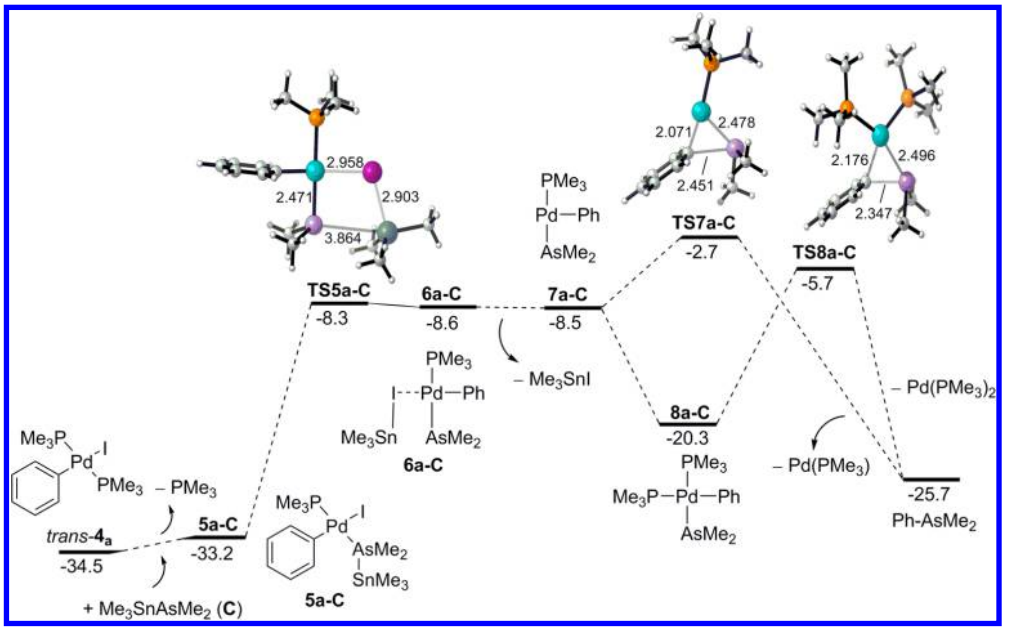


**Figure 7.** Computed reaction profile and ball-and-stick representations of the species involved in the transmetalation and reductive elimination steps for the catalytic cycle of the Stille cross-coupling reaction of PhI (**1a**) and $Me_3SnAsMe_2$ catalyzed by $Pd(PMe_3)_2$. Relative free energies ($\Delta G_{298}$, at 298.15 K) are given in kcal/mol. Bond distances are given in angstroms. All data have been computed at the PCM(toluene)-B3LYP-D3/6-311+G(d)&SDD//B3LYP/6-31+G(d)&SDD level.

activation barriers for the transmetalation process increase in the order X = Cl < Br < I.[20] This effect was ascribed to the fact that the Sn−X bond energy increases faster than the Pd−X bond energy in the order X = I < Br < Cl.[20]

Results above indicate that the effect of the halide on the transmetalation step involving heterostannanes can be considered as negligible. Therefore, the origins of the observed lack of reactivity necessarily should be found in the previous oxidation addition step. As expected, the computed activation barrier for the oxidative addition of PhCl (**1b**) to $PdL_2$ through **TS2b** ($\Delta G^{\ddagger}_{298}$ = 23.6 kcal/mol) is considerably higher than that computed for the process involving PhI ($\Delta G^{\ddagger}_{298}$ = 12.8 kcal/mol, see Figure 2). This agrees with previous computational reports,[12b,21] and it can be directly ascribed to the relative $C_{aryl}$−X bond strength, which manifests itself in a less destabilizing activation strain energy,[16] according to the so-called activation strain model (ASM) of reactivity.[22]

Alternatively, the involvement of 12-electron species PdL instead of $PdL_2$ has been suggested as the active catalytic species, particularly in the reactions involving chlorobenzenes.[15a,23,24] Despite that, our calculations indicate that the activation barrier is even higher for the process involving the monocoordinated species (via **TS2b-M**, $\Delta G^{\ddagger}_{298}$ = 28.7 kcal/mol). Therefore, we can conclude that the observed lack of reactivity of aryl chlorides with heterostannanes finds its origin in the initial oxidative addition step and not during the subsequent transmetalation reaction.

**Effect of the Substituents Attached to the Heteroatom.** To complete this study, we decided to investigate the effect of an alkyl substituent instead of an aryl fragment directly attached to the heteroatom of the stannane to computationally explore the feasibility of the process. To this end, the two-step transmetalation reaction and the subsequent reductive elimination involving the model $Me_3SnAsMe_2$ heterostannane have been computed.

The corresponding reaction profile is depicted in Figure 7. The initial $PMe_3$ by $Me_3SnAsMe_2$ ligand interchange is again slightly endergonic ($\Delta G_{R,298}$ = +1.3 kcal/mol) due to the stabilization of the As lone pair ($E_{HOMO}$ = −5.90 eV), which resembles the analogous reaction step involving $Me_3SnAsPh_2$ (see Figure 2). The computed activation barrier for the transmetalation reaction involving **TS5a-C** ($\Delta G^{\ddagger}_{298}$ = 24.9 kcal/mol) is higher than that for the process involving **TS5a-As** ($\Delta G^{\ddagger}_{298}$ = 23.2 kcal/mol) as a consequence of the stronger As−Sn bond in **5a-C** as compared to **5a-As** (corresponding WBI: 0.73 vs 0.69). This transformation leads to the weakly bonded complex **6a-C**, which readily evolves to **7a-C**, releasing $Me_3SnI$ again in an endergonic transformation. At variance, the final reductive elimination, which takes place through the transition state **TS7a-C**, proceeds with a much lower activation barrier ($\Delta G^{\ddagger}_{298}$ = 5.8 kcal/mol vs $\Delta G^{\ddagger}_{298}$ = 11.2 kcal/mol) in a exergonic transformation ($\Delta G_{R,298}$ = −17.2 kcal/mol). Inspection of the corresponding transition states **TS7a-C** (Figure 7) and **TS7a-As** (Figure 4) clearly indicates that the reductive elimination involving the $AsMe_2$ fragment proceeds via an earlier transition state than the analogous process involving $AsPh_2$. This becomes obvious when comparing the relevant bond lengths in both saddle points: while the Pd···As and Pd···C distances are clearly shorter (thus indicating a more reactant-like transition state) in **TS7a-C**, the As···C distance is clearly longer (therefore indicating a more product-like transition state for **TS7a-As**). Finally, and similar to the results stated above, the reductive elimination through the tetracoordinated intermediate **8a-C** is competitive in view of the exergonicity associated with the initial coordination of the $PMe_3$ ($\Delta G_{R,298}$ = −11.8 kcal/mol) ligand and the relatively low barrier ($\Delta G^{\ddagger}_{298}$ = 14.6 kcal/mol) computed for the process involving the three-membered cyclic transition state **TS8a-C**.

Taking into account these computational results, we can conclude that the replacement of phenyl groups by alkyl groups in the heterostannane $Me_3SnAsR_2$ slightly increases the activation barrier for the transmetalation step and leads to a much more kinetically favored final reductive elimination.


DOI: 10.1021/om501027s
Organometallics XXXX, XXX, XXX−XXX

Therefore, our calculations predict that this process should be experimentally feasible.

## CONCLUSIONS

From the computational study reported herein, the following conclusions can be drawn:

(1) The Stille reaction involving aryl halides (PhCl, PhI) and heterostannanes ($Me_3SnZR_2$, Z = As, P; R = Ph, Me) proceeds according to the typical Stille three-step mechanism, i.e., oxidative addition, transmetalation, and final reductive elimination.

(2) The transmetalation reaction occurs via the so-called cyclic mechanism in view of the quite high endergonicity ($\Delta G_{R,298} \approx 30-35$ kcal/mol) computed for the initial phosphine/halide ligand interchange required for the alternative open mechanism.

(3) The overall relative reaction profile for the transmetalation involving $Me_3SnPPh_2$ is always more energetically favored than that involving $Me_3SnAsPh_2$, which nicely agrees with the experimental observations.

(4) The observed higher reactivity of the phosphorus heterostannane can be ascribed to the relative strength of the Sn−Z bond, which is broken during the transmetalation step (Sn−P < Sn−As).

(5) The origin of the lack of reactivity of aryl chlorides in the analogous Stille coupling with heterostannanes is found in the initial oxidative addition reaction (the subsequent transmetalation and reductive elimination processes being quite similar to those involving aryl iodides).

(6) With the notable exception of the lower barrier computed for the final reductive elimination step, no significant differences have been found for the process involving the alkyl-substituted stannane $Me_3SnAsMe_2$, therefore suggesting that this transformation should be experimentally feasible.

## COMPUTATIONAL DETAILS

All the calculations reported in this paper were obtained with the Gaussian 09 suite of programs.[25] Electron correlation was partially taken into account using the hybrid functional usually denoted as B3LYP,[26] using the SDD (Stuttgart/Dresden)[27] effective core potential for Pd, Sn, and I and the double-$\zeta$ quality plus polarization 6-31+G(d) basis set for all other elements. Reactants and products were characterized by frequency calculations[28] and have positive definite Hessian matrices. Transition structures show only one negative eigenvalue in their diagonalized force constant matrices, and their associated eigenvectors were confirmed to correspond to the motion along the reaction coordinate under consideration using the intrinsic reaction coordinate (IRC) method in specific cases.[29] Solvents effects were taken into account using the polarizable continuum model (PCM).[30] Single-point calculations on the gas-phase-optimized geometries were performed to estimate the change in the Gibbs energies in the presence of toluene as solvent using the triple-$\zeta$ quality 6-311+G(d) basis set including the SDD for Pd, Sn, and I. In addition, dispersion effects have been considered using the D3 dispersion correction suggested by Grimme et al.[31] This level is denoted PCM(toluene)-B3LYP-D3/6-311+G(d)&SDD//B3LYP/6-31+G(d)&SDD. The $\Delta G$ values given in the text were obtained from the Gibbs energy in solution, $G_{sol}$, which was calculated by adding the thermochemistry corrections, $G - E$, to the refined single-point energies, $E_{sol}$, i.e., $G_{sol} = E_{sol} + G - E$. Wiberg bond indices have been computed using the natural bond orbital (NBO) method.[32]

## ASSOCIATED CONTENT

### Supporting Information

Figure 1S and Cartesian coordinates and total energies of all the stationary points discussed in the text. This material is available free of charge via the Internet at http://pubs.acs.org.

## AUTHOR INFORMATION

### Corresponding Authors

*E-mail: israel@quim.ucm.es.

*E-mail: martins@fcq.unc.edu.ar.

### Notes

The authors declare no competing financial interest.

## ACKNOWLEDGMENTS

S.E.M. and E.D.S.C. thank CONICET (PIP-00683), FONCYT (PICT-2012-2303), and SECYT-Universidad Nacional de Córdoba (05/CP15) for their continuous support of the work. I.F. acknowledges research support from the Spanish MINECO and European FEDER (CTQ2013-44303-P and Consolider-Ingenio 2010, CSD2007-00006 grants).

## REFERENCES

(1) (a) Diederich, F.; de Meijere, A., Eds. *Metal-Catalyzed Cross-Coupling Reaction*, 2nd ed.; Wiley-VCH: Weinheim, 2004; Vols. *1 and 2*. (b) Johansson Seechurn, C. C. C.; Kitching, M. O.; Colacot, T. J.; Snieckus, V. *Angew. Chem., Int. Ed.* **2012**, *51*, 5062−5085. (c) Magano, J.; Dunetz, J. R. *Chem. Rev.* **2011**, *111*, 2177−2250. (d) Suzuki, A. *Angew. Chem., Int. Ed.* **2011**, *50*, 6722−6737. (e) Nicolaou, K. C.; Bulger, P. G.; Sarlah, D. *Angew. Chem., Int. Ed.* **2005**, *44*, 4442−4489. (f) Corbet, J.-P.; Mignani, G. *Chem. Rev.* **2006**, *106*, 2651−2710.

(2) For reviews of the Stille reaction see: (a) Espinet, P.; Echavarren, A. M. *Angew. Chem., Int. Ed.* **2004**, *43*, 4704−4734. (b) Pascual, S.; Echavarren, A. M. In *Tin Chemistry*; Davies, A. G., Ed.; John Wiley & Sons Ltd.: Chichester, 2008; pp 579−606. (c) Pengand, Y.; Li, W.-D. Z. *Eur. J. Org. Chem.* **2010**, 6703−6718.

(3) (a) Lord, A.-M.; Mahon, M. F.; Lloyd, M. D.; Threadgill, M. D. *J. Med. Chem.* **2009**, *52*, 868−877. (b) Amans, D.; Bellosta, V.; Cossy, J. *Org. Lett.* **2007**, *9*, 4761−4764. (c) Uchil, V.; Seo, B.; Nair, V. *J. Org. Chem.* **2007**, *72*, 8577−8579.

(4) Recent applications in natural products total synthesis: (a) Masters, K.-S.; Flynn, B. L. *Org. Biomol. Chem.* **2010**, *8*, 1290−1292. (b) Tang, B.; Bray, C. D.; Pattenden, G.; Rogers, J. *Tetrahedron* **2010**, *66*, 2492−2500. (c) Candy, M.; Audran, G.; Bienayme, H.; Bressy, C.; Pons, J.-M. *J. Org. Chem.* **2010**, *75*, 1354−1359. (d) Amans, D.; Bareille, L.; Bellosta, V.; Cossy, J. *J. Org. Chem.* **2009**, *74*, 7665−7674. (e) Sofiyev, V.; Navarro, G.; Trauner, D. *Org. Lett.* **2008**, *10*, 149−152.

(5) (a) Carsten, B.; He, F.; Son, H. J.; Xu, T.; Yu, L. *Chem. Rev.* **2011**, *111*, 1493−1528. (b) Song, C.; Swager, T. M. *Macromolecules* **2009**, *42*, 1472−1475. (c) Qi, T.; Liu, Y.; Qiu, W.; Zhang, H.; Gao, X.; Liu, Y.; Lu, K.; Du, C.; Yu, G.; Zhu, D. *J. Mater. Chem.* **2008**, *18*, 1131−1138. (d) Gau, J.; Li, L.; Meng, Q.; Li, R.; Jiang, H.; Li, H.; Hu, W. *J. Mater. Chem.* **2007**, *17*, 1421−1426.

(6) For some examples in C−N bond formation, see: (a) Kim, Y. O.; Yu, S. *J. Am. Chem. Soc.* **2003**, *125*, 1696−1697. (b) Koza, D. J.; Nsiah, Y. A. *J. Org. Chem.* **2002**, *67*, 5025−5027. (c) Paul, F.; Hartwing, J. F. *J. Am. Chem. Soc.* **1994**, *116*, 5969−5970. For C−Se see: (d) Nishiyama, Y.; Sonoda, N. *Mini-Rev. Org. Chem.* **2005**, *2*, 147−155. (e) Nishiyama, Y.; Kawamatsu, H.; Funato, S.; Tokunaga, K.; Sonoda, N. *J. Org. Chem.* **2003**, *68*, 3599−3602. (f) Beletskaya, I. P.; Sigeev, A. S.; Peregudov, A. S.; Petrovskii, P. V. *J. Organomet. Chem.* **2000**, *605*, 96−101. (g) Wallner, O. A.; Szabó, K. M. *J. Org. Chem.* **2005**, *70*, 9215−9221. For C−P see: (h) Tunney, S. E.; Stille, J. K. *J. Org. Chem.* **1987**, *52*, 748−753. For C−S, C−Si, and C−Sn see: (i) Rossi, R. A.; Martín, S. E. *Coord. Chem. Rev.* **2006**, *250*, 575−601.



DOI: 10.1021/om501027s
*Organometallics* XXXX, XXX, XXX−XXX

(7) (a) Martín, S. E.; Bonaterra, M.; Rossi, R. A. *J. Organomet. Chem.* **2002**, *664*, 223−227. (b) Bonaterra, M.; Martín, S. E.; Rossi, R. A. *Tetrahedron Lett.* **2006**, *47*, 3511−3515. (c) Bonaterra, M.; Rossi, R. A.; Martín, S. E. *Organometallics* **2009**, *28*, 933−936. (d) Lanteri, M. N.; Rossi, R. A.; Martín, S. E. *J. Organomet. Chem.* **2009**, *694*, 3425−3430.

(8) (a) Bonaterra, M.; Martín, S. E.; Rossi, R. A. *Org. Lett.* **2003**, *15*, 2731−2734. (b) Uberman, P. M.; Lanteri, M. N.; Martín, S. E. *Organometallics* **2009**, *28*, 6927−6934.

(9) (a) Uberman, P. M.; Parajón Puenzo, S. C.; Lanteri, M. N.; Martín, S. E. *Dalton Trans.* **2011**, *40*, 9229−9237. (b) Uberman, P. M.; Caira, M. R.; Martín, S. E. *Organometallics* **2013**, *32*, 3220−3226.

(10) Stille, J. K. *Angew. Chem., Int. Ed.* **1986**, *25*, 508−524.

(11) For selected examples, see: (a) Casado, A. L.; Espinet, P. J.; Gallego, A. M. *J. Am. Chem. Soc.* **2000**, *122*, 11771−11782. (b) Casado, A. L.; Espinet, P.; Gallego, A. M.; Martínez-Ilarduya, J. M. *Chem. Commun.* **2001**, 339−340. (c) Casares, J. A.; Espinet, P.; Salas, G. *Chem.—Eur. J.* **2002**, *8*, 4843−4853. (d) Nilsson, P.; Puxty, G.; Wendt, O. F. *Organometallics* **2006**, *27*, 1285−1292. (e) Santos, L. S.; Rosso, G. B.; Pilli, R. A.; Eberlin, M. N. *J. Org. Chem.* **2007**, *72*, 5809−5812. (f) Pérez-Temprano, M. H.; Nova, A.; Casares, J. A.; Espinet, P. *J. Am. Chem. Soc.* **2008**, *130*, 10518−10520. (g) Verbeeck, S.; Meyers, C.; Franck, P.; Jutand, A.; Maes, B. U. W. *Chem.—Eur. J.* **2010**, *16*, 12831−12837. (h) Pérez Temprano, M. H.; Gallego, A. M.; Casares, J. A.; Espinet, P. *Organometallics* **2011**, *30*, 611−617.

(12) For recent reviews, see: (a) Xue, L.; Lin, Z. *Chem. Soc. Rev.* **2010**, *39*, 1692−1705. (b) García-Melchor, M.; Braga, A. A. C.; Lledós, A.; Ujaque, G.; Maseras, F. *Acc. Chem. Res.* **2013**, *46*, 2626−2634.

(13) (a) Casado, A. L.; Espinet, P. *J. Am. Chem. Soc.* **1998**, *120*, 8978−8985. (b) Amatore, C.; Pfluger, F. *Organometallics* **1990**, *9*, 2276−2282. (c) Amatore, C.; Azzabi, M.; Jutand, A. *J. Organomet. Chem.* **1989**, *363*, C41−C45. (d) Shekhar, S.; Ryberg, P.; Hartwig, J. F.; Mathew, J. S.; Blackmond, D. G.; Strieter, E. R.; Buchwald, S. L. *J. Am. Chem. Soc.* **2006**, *128*, 3584−3591. (e) Santos, L. S.; Rosso, G. B.; Pilli, R. A.; Eberlin, M. N. *J. Org. Chem.* **2007**, *72*, 5809−5812.

(14) (a) Goossen, L. J.; Koley, D. H.; Hermann, H. L.; Thiel, W. *Organometallics* **2006**, *25*, 54−67. (b) Ahlquist, M.; Norrby, P.-O. *Organometallics* **2007**, *26*, 550−553. (c) Schoenebeck, F.; Houk, K. N. *J. Am. Chem. Soc.* **2010**, *132*, 2496−2497. (d) Lam, K. C.; Marder, T. B.; Lin, Z. Y. *Organometallics* **2007**, *26*, 758−760. (e) McMullin, C. L.; Jover, J.; Harvey, J. N.; Fey, N. *Dalton Trans.* **2010**, *39*, 10833−10836.

(15) Similar reaction energies have been computed for related oxidative additions. See, for instance: (a) Braga, A. C. A.; Ujaque, G.; Maseras, F. *Organometallics* **2006**, *25*, 3647−3658. (b) Fernández, I.; Solé, D.; Sierra, M. A. *J. Org. Chem.* **2011**, *76*, 1592−1598.

(16) For a discussion on the concerted vs the alternative $S_N2$ reaction pathways, see: Fernández, I.; Bickelhaupt, F. M. *Chem. Soc. Rev.* **2014**, *43*, 4953−4967 and reference 12b.

(17) (a) Álvarez, R.; Faza, O. N.; López, C. S.; de Lera, A. R. *Org. Lett.* **2006**, *8*, 35−38. (b) Nova, A.; Ujaque, G.; Maseras, F.; Lledós, A.; Espinet, P. *J. Am. Chem. Soc.* **2006**, *128*, 14571−14578. (c) Álvarez, R.; Pérez, M.; Faza, O. N.; de Lera, A. R. *Organometallics* **2008**, *27*, 3378−3389.

(18) Álvarez, R.; Faza, O. N.; de Lera, A. R.; Cárdenas, D. J. *Adv. Synth. Catal.* **2007**, *349*, 887−906.

(19) Pérez-Rodríguez, M.; Braga, A. A. C.; García-Melchor, M.; Pérez-Temprano, M. H.; Casares, J. A.; Ujaque, G.; de Lera, A. R.; Álvarez, R.; Maseras, F.; Espinet, P. *J. Am. Chem. Soc.* **2009**, *131*, 3650−3657.

(20) Ariafard, A.; Lin, Z.; Fairlamb, J. S. *Organometallics* **2006**, *25*, 5788−5794.

(21) (a) van Zeist, W.-J.; Bickelhaupt, F. M. *Dalton Trans.* **2011**, *40*, 3028−3038. and references therein. See also: (b) Fernández, I.; Wolters, L. P.; Bickelhaupt, F. M. *J. Comput. Chem.* **2014**, *35*, 2140−2145.

(22) For recent reviews on the ASM method, see: (a) van Zeist, W.-J.; Bickelhaupt, F. M. *Org. Biomol. Chem.* **2010**, *8*, 3118−3127. (b) Fernández, I. *Phys. Chem. Chem. Phys.* **2014**, (*16*), 7662−7671 and ref 16. See also: (c) Fernández, I. *Understanding Trends in Reaction Barriers in Discovering the Future of Molecular Sciences*; Pignataro, B., Ed.; Wiley-VCH: Weinheim, 2014; pp 165−187.

(23) (a) Christmann, U.; Vilar, R. *Angew. Chem., Int. Ed.* **2005**, *44*, 366−374. (b) Barrios-Landeros, F.; Hartwig, J. F. *J. Am. Chem. Soc.* **2005**, *127*, 6944−6945. (c) Barder, T. E.; Biscoe, M. R.; Buchwald, S. L. *Organometallics* **2007**, *26*, 2183−2192. (d) Li, Z.; Fu, Y.; Guo, Q.-X.; Liu, L. *Organometallics* **2008**, *27*, 4043−4049. (e) Ahlquist, M.; Fristrup, P.; Tanner, D.; Norrby, P.-O. *Organometallics* **2006**, *25*, 2066−2073.

(24) Vidossich, P.; Ujaque, G.; Lledós, A. *Chem. Commun.* **2014**, *50*, 661−663.

(25) Frisch, M. J.; Trucks, G. W.; Schlegel, H. B.; Scuseria, G. E.; Robb, M. A.; Cheeseman, J. R.; Scalmani, G.; Barone, V.; Mennucci, B.; Petersson, G. A.; Nakatsuji, H.; Caricato, M.; Li, X.; Hratchian, H. P.; Izmaylov, A. F.; Bloino, J.; Zheng, G.; Sonnenberg, J. L.; Hada, M.; Ehara, M.; Toyota, K.; Fukuda, R.; Hasegawa, J.; Ishida, M.; Nakajima, T.; Honda, Y.; Kitao, O.; Nakai, H.; Vreven, T.; Montgomery, J. A., Jr.; Peralta, J. E.; Ogliaro, F.; Bearpark, M.; Heyd, J. J.; Brothers, E.; Kudin, K. N.; Staroverov, V. N.; Kobayashi, R.; Normand, J.; Raghavachari, K.; Rendell, A.; Burant, J. C.; Iyengar, S. S.; Tomasi, J.; Cossi, M.; Rega, N.; Millam, N. J.; Klene, M.; Knox, J. E.; Cross, J. B.; Bakken, V.; Adamo, C.; Jaramillo, J.; Gomperts, R.; Stratmann, R. E.; Yazyev, O.; Austin, A. J.; Cammi, R.; Pomelli, C.; Ochterski, J. W.; Martin, R. L.; Morokuma, K.; Zakrzewski, V. G.; Voth, G. A.; Salvador, P.; Dannenberg, J. J.; Dapprich, S.; Daniels, A. D.; Farkas, Ö.; Foresman, J. B.; Ortiz, J. V.; Cioslowski, J.; Fox, D. J. *Gaussian 09*, Revision B.01; Gaussian, Inc.: Wallingford, CT, 2009.

(26) (a) Becke, A. D. *J. Chem. Phys.* **1993**, *98*, 5648−5652. (b) Lee, C.; Yang, W.; Parr, R. G. *Phys. Rev. B* **1988**, *37*, 785−789. (c) Vosko, S. H.; Wilk, L.; Nusair, M. *Can. J. Phys.* **1980**, *58*, 1200−1211.

(27) (a) Dunning, T. H., Jr.; Hay, P. J. In *Modern Theoretical Chemistry*; Schaefer, H. F., III, Ed.; Plenum: New York, 1976; Vol. 3. (b) Leininger, T.; Nicklass, A.; Stoll, H.; Dolg, M.; Schwerdtfeger, P. *J. Chem. Phys.* **1996**, *105*, 1052−1059.

(28) McIver, J. W.; Komornicki, A. K. *J. Am. Chem. Soc.* **1972**, *94*, 2625−2633.

(29) González, C.; Schlegel, H. B. *J. Phys. Chem.* **1990**, *94*, 5523−5527.

(30) (a) Miertuš, S.; Scrocco, E.; Tomasi, J. *Chem. Phys.* **1981**, *55*, 117−129. (b) Pascual-Ahuir, J. L.; Silla, E.; Tuñón, I. *J. Comput. Chem.* **1994**, *15*, 1127−1138. (c) Barone, V.; Cossi, M. *J. Phys. Chem. A* **1998**, *102*, 1995−2001.

(31) Grimme, S.; Antony, J.; Ehrlich, S.; Krieg, H. *J. Chem. Phys.* **2010**, *132*, 154104−154119.

(32) (a) Foster, J. P.; Weinhold, F. *J. Am. Chem. Soc.* **1980**, *102*, 7211−7218. (b) Reed, A. E.; Weinhold, F. *J. Chem. Phys.* **1985**, *83*, 1736−1740. (c) Reed, A. E.; Weinstock, R. B.; Weinhold, F. *J. Chem. Phys.* **1985**, *83*, 735−746. (d) Reed, A. E.; Curtiss, L. A.; Weinhold, F. *Chem. Rev.* **1988**, *88*, 899−926.



DOI: 10.1021/om501027s
*Organometallics* XXXX, XXX, XXX−XXX